JERZY MALACHOWSKI [*], VOLODYMYR HUTSAYLYUK [**], PETR YUKHUMETS [***], ROMAN DMITRYENKO [***], GRIGORII BELIAIEV [***], IHOR PRUDKII [***]

INVESTIGATION OF THE STRESS-STRAIN STATE OF SEAMLESS PIPE IN THE INITIAL STATE

Mechanical properties of the pipeline samples that had been cut in annular and axial directions were investigated. The methodology of modeling and calculation of the real stress-strain state was described. The stable state during in the deformation process was defined. The results of the experimental researches were used as a test variant during examination of pipe strength.

1. Introduction

Pipeline systems are important for effective functioning of the industry and as well as for providing the needs of the population with essential energy resources: oil, natural gas, liquid petroleum, etc. An extensive network of pipelines, both local and internationally are supporting vital functions and economic development. Destruction of even small sections of the pipeline could have cause serious consequences. Breakdown of pipelines is often accompanied by explosions and fires. Total damages would result in cost-concerned with a loss of gas and petroleum products, high costs of the repair and breaking cutting the gas supply. The last one may be particularly noticeable due to the fact that pipelines are usually located at the areas remote from settlements, which increases the time of the repair. Moreover,

[*] *Military University of Technology, Faculty of Mechanical Engineering, Department of Mechanics and Applied Computer Science, Gen. S. Kaliskiego 2. St., 00-908 Warsaw, Poland; E-mail: jerzy.malachowski@wat.edu.pl*

[**] *Military University of Technology, Faculty of Mechanical Engineering, Department of Machine Design, Gen. S. Kaliskiego 2. St., 00-908 Warsaw, Poland; E-mail: vhutsaylyuk@wat.edu.pl*

[***] *The E.O.Paton Electric Welding Institute, Department of new structural forms of welded structures and designs, No.12, Bozhenko 17.St., Kiev, Ukraine; E-mail: yupeter@ukr.net*

by increasing pipe diameter and operating pressure in case of an accident it can lead to a significant environmental pollution caused as a result from a spill of large volumes of oil or gas.

Considering life-time of the pipeline and the fact that more than 20% of the pipes active service life will be expired shortly, the problem of investigating the causes of failure of the transport systems is becoming increasingly important.

A failure of the bearing elements of piping systems occurs for a variety of reasons. It depends on the design of the elements, features of their work and loading, and physical-mechanical properties of the base material, etc. [1]. The main pipeline remains in a complex stress state under high internal pressure, temperature difference, uneven ground pressure, elastic distortions that result from the rugged topography, soil impacts associated with changes in its structure-swelling, drawdown, etc. These factors cause stresses from bending with stretching or bending with compression in the pipeline.

One of the main criteria that determine the reliability of pipelines are the parameters of ultimate deformation. The change in the stress-strain state (SSS) to the level of metal plastic deformation leads to a change in geometry of the pipe and weakens the overall strength of the construction. Problem of investigating the real stress-strain state is that, a pipeline is under the influence of multiaxial stresses, which change during operation time. Definition of all real values stresses for the mathematical design is not always possible. Generally, for design of strength of the material in these cases, used a simplified scheme [2], where the stresses are measured in two planes of measurement.

2. Experimental and design works

The object of investigation of this article is the seamless hot pipe produced by "INTERPIPE Nizhnedneprovsky TRUBOPRAKATNY PLANT." Its certificate is as follows: pipe $N^{\underline{o}}$ 443, smelting number 32416, diameter 219 mm, wall thickness 6 mm, weight per meter ~33.51 kg, Steel 20. A certificate of pipe quality corresponds to GOST 8732-78 and GOST 8731-74. The mechanical properties and chemical composition are shown in Table 1 and Table 2, respectively.

Table 1.

Mechanical properties

	σ, MPa	$\sigma_{0.2}$, MPa	$\delta, \%$	Flattening
Melt $N^{\underline{o}}$ 32416	475.78	323.73	32.0	satisfactory
	480.69	328.64	33.0	satisfactory

Table 2.

Chemical composition

	C, %	Mn, %	Si, %	S, %	P, %	Cr, %	Ni, %	Cu, %
Certificate(Melt N° 32416)	0.19	0.54	0.29	0.02	0.011	0.07	0.05	0.08
Measured (lab. EWI).	0.177	0.55	0.289	0.018	0.008	0.078	0.065	0.070

Mechanical tensile tests were carried out on samples in the initial state (state of delivery). At least five selected samples were cut from tube N° 443 in the annular and axial directions (Fig. 1).
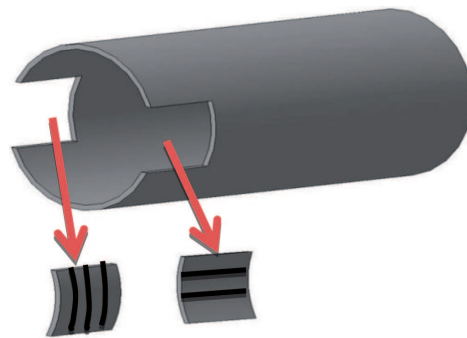

Fig. 1. Schematic representation of the pipe

The first batch of samples consisted of four pieces cut in the circumferential direction. Two of them were straightened on a press, and the other two were not rectified with a working part. Only the place under the grips was aligned (Fig. 2a). The second batch consisted of two samples cut in the axial direction. The surface of the samples was not treated. The tests were conducted at the GS Pisarenko Institute for Problems of Strength of NASU.
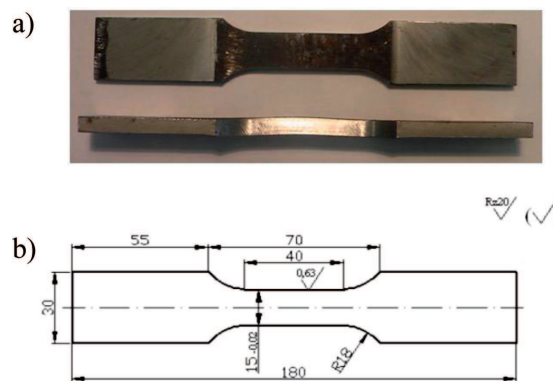

Fig. 2. Photo (a) and schematic illustration (b) of samples cut in the circumferential direction

The deformations in tensile specimens were defined through readings of movements recorded by a strain sensor. The sensor was mounted on the working parts of the samples. The strain sensor base was 25 mm. To measure the residual deformation of the samples, the base of length of approximately 40 mm was used (Fig. 3). The cross-section area of the samples was about 103 mm^2.
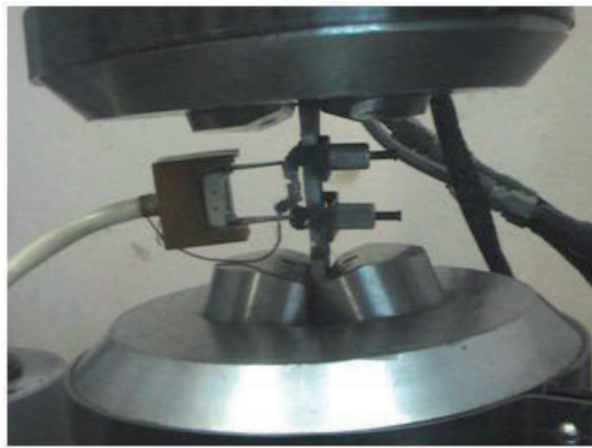

Fig. 3. Photo of the strain sensor mounted on the sample

During the mechanical test of the specimen a tension curve $\bar{\sigma}$, $\bar{\varepsilon}$ was prepared, where $\bar{\sigma}$ – stress calculated as the quotient of force on the area of cross-section sample in origin state, and $\bar{\varepsilon} = \Delta l/l_0$ regular longitudinal deformation of the specimen, defined as base elongation divided by the length of the base stamped on the working part. The maximum stress that was realized was called the temporary resistance. Before this value is reached, the specimen deforms uniformly, after that a neck is formed.

For application of the test results, not only in the case of a uniaxial stress state, but also for the SSS, from standard curve of tension $\bar{\sigma}$, $\bar{\varepsilon}$ get real curve of tension σ_r, ε_r (1, 2). This assertion is valid only until the moment when neck starts to form:

$$\varepsilon_r = \ln\left(1 + \bar{\varepsilon}\right), \quad \sigma_r = \bar{\sigma}\left(1 + \bar{\varepsilon}\right) \tag{1}$$

During the formation of the neck, a multiaxial stress state develops, which depends on the geometric shape of the specimen. The next curve is transformed into the so-called real strain curve – σ_i, ε_i by applying formula (3) [3]:

$$\varepsilon_i = \varepsilon_r - \frac{1 - 2\mu}{3E}\sigma_r, \quad \sigma_i = \sigma_r \tag{2}$$

where μ is the Poisson's ratio.

In the elastic region, the Poisson's ratio is about 0.3. Its further change is defined by formula (3). However, the increase is observed only at the initial stage prior to the yield strength $\varepsilon_{i0.2}$. It results from generation of new sources of dislocation and an increase in their density [7]. An example of calculation of Poisson's ratio μ through $\bar{\sigma}$, $\bar{\varepsilon}$, is shown in Figs 4a and 4b.

$$\mu = \frac{1}{2} - \frac{1 - 2\mu_e}{2E} \frac{\sigma_r}{\varepsilon_r} \tag{3}$$

where μ_e, E − coefficient and modulus of elasticity in the range.

Residual deformation after the destruction of the sample was measured on two different bases including a neck. This makes possible to determine residual deformation for any base length. Outside the neck, which takes a significant part of the deformation, the sample is deformed unevenly, and the strain does not correspond to the tensile strength. As it is known, for the values greater than $\bar{\sigma}_u$, the force that stretches the sample begins to fall.

With the increasing base, the residual deformation will tend to become uniform and in infinity they will be equal mutually. Very significant deformation concentrates in the center of the neck, measurements in this place have not been conducted.

The thin-walled cylindrical and spherical shells lose their ability to sustainable uniform deformation, where their internal pressure does not increases ($dp = 0$) [8]. When shell wall local thinning takes place, it results in the loss of stability of the original form and initial equilibrium of construction.

3. Results and Discussion

Figure 4a shows the tension curve obtained from the experimental data and adapted her for real stresses and strain in axial and ring samples. In the lower part figure, there is shown the calculated change in Poisson's ratio [3]. It is worth noting that its initial value is 0.3. Curves are obtained up to start forming neck. Figure 4b present the tension curve and the calculated value of Poisson's ratio up to 0.05% strain.

Points on the tensile diagram correspond to the maximum value (Fig. 4). They present horizontal part on the real curves, respectively.

Elastic deformation (indicated by E in the figure) was obtained on the assumption that the modulus of elasticity $E = 2 \cdot 10^5$ MPa. For circumferential and axial specimens, the proportional limit corresponds to the value of the order of 200 MPa.

Relations rate of strain from the level of deformation is shown in Fig. 5a. Relations of the deformation time, from the level of deformation is shown in Fig. 5b. Tensile strain rate was defined as $\Delta\bar{\varepsilon}/\Delta t$ and plotted as a function
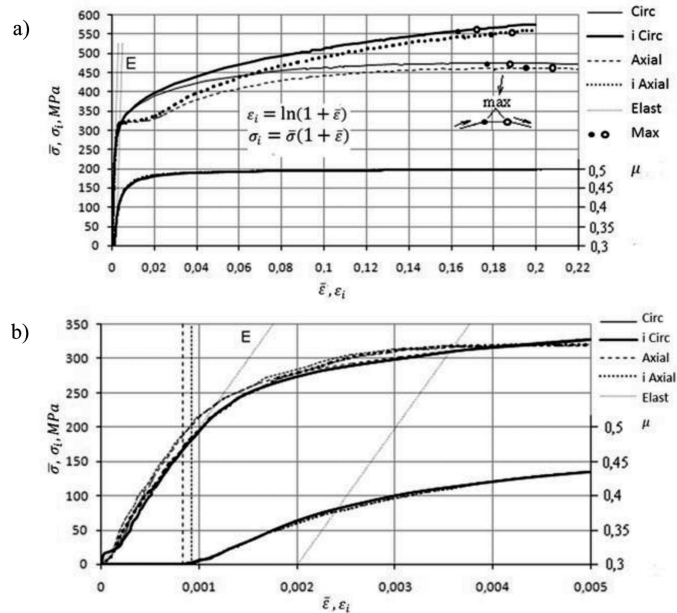
Fig. 4. Stress-strain diagrams $\bar{\sigma}, \bar{\varepsilon}$, actual diagram σ_i, ε_i in the ring and axial directions, μ – change of Poisson's ratio to 22% strain (a), up to 0.05% strain (b)
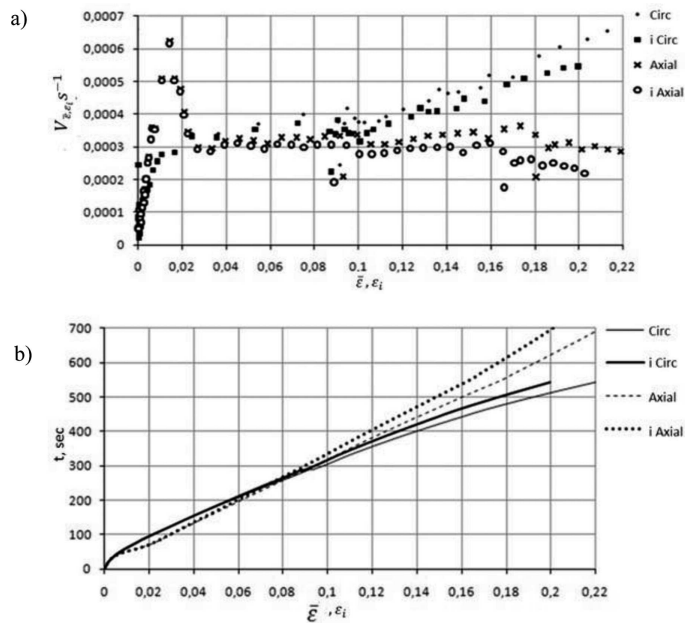

Fig. 5. Strain rate dependence (a) and time plastic deformation (b) from degree of deformation $\bar{\varepsilon}$, ε_i

of $\bar{\varepsilon}$. Strain rate, defined as $\Delta\varepsilon_i/\Delta t$ and built according to ε_i corresponds to real values. The curves are obtained up to strain values of 22%.

Extension rate of the working parts of the samples in the elastic region, before the formation of neck occurred, was less than $2 \cdot 10^{-4}$, $3 \cdot 10^{-4}$, $7 \cdot 10^{-4}$ s^{-1} for the circular sample and $2 \cdot 10^{-4}$, $6 \cdot 10^{-4}$, $4 \cdot 10^{-4}$ s^{-1} for the axial sample. In the initial part of the plastic deformation for the axial sample, the yield plateau is observed.

Figure 6 shows the partial curves built for the circular and axial samples with the strain of not greater than 5%. The number of measurements performed by the strain sensor is about 12 measurements in the first 5 seconds of stretching and 12 measurements in the last 100 seconds. The total number of measurements for the axial sample is 103 and 116 for the circular one.
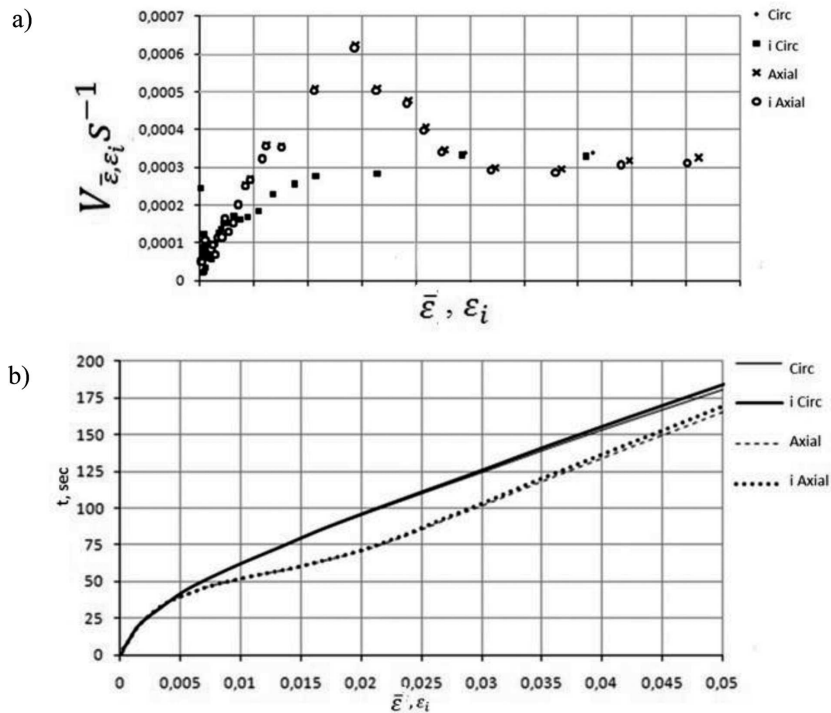

Fig. 6. Relations of strain rate (a) and time of plastic deformation (b) from level of deformation in the interval deformation 0–5%

The graphs show that the pipe in both circular and axial directions indicates peculiar anisotropy. If the curves obtained for the circular direction moves to the right direction by 0.02, they approximately will be the same with the curves obtained from the axial direction. In the circular direction, the pipe deformed up to 2%, which is associated with its production. It is known that after the manufacturing process, an internal pressure test was not carried out.

Table 3 shows the mechanical properties obtained by testing tensile specimens.

The mechanical properties obtained by testing tensile specimens

	Ring samples				Axial samples (III)	
	Deformation working part (I)		Without deformation working part (II)			
	a	b	a	b*	a*	b
$\bar{\sigma}_y$, MPa					320	320
$\bar{\sigma}_{0.2}$, MPa	320	327	315	308.5		
$\bar{\sigma}_u$, MPa	473.21	475.5	479.34	474.76	462.39	466.67
δ, % along base of extensometer	–	38.99	35.96	41.04	–	44.79
δ, % along base of sample	26.76	33.35	33.77	33.13	40.97	37.73
δ, % uniform deformation	13.9	20.3	17.2	18.6	21.2	18.8
ψ, % relative reduction	44.52	50.79	48.98	48.24	54.6	54.9

* – samples for constructing curves. Base of stress sensor – 25 mm. Base of sample – 41 mm.

Table 3 shows that for both directions "yield stress" $\bar{\sigma}_{0.2}$ and tensile strengths $\bar{\sigma}_u$ are the same. Figure 7 shows the stress-strain curve of six samples.
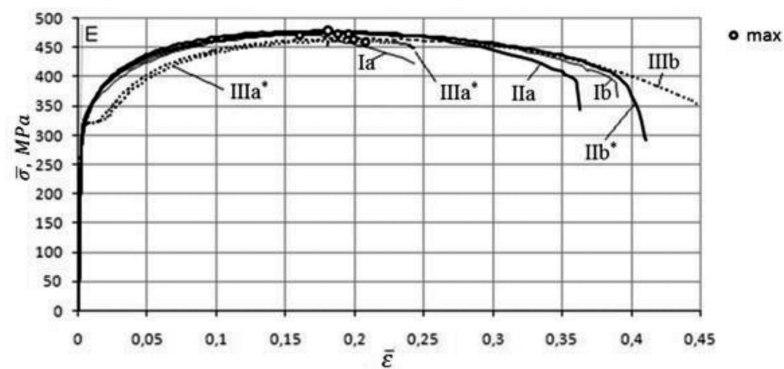

Fig. 7. The stress-strain curve of six samples. On the descending part of the curve of samples Ia and IIIa*, stress sensor was removed

Determination of the steady state during the deformation was carried out according to the method of calculation for thin-walled cylindrical and spherical shells loaded by internal pressure. For this purpose, the curve data σ_i, ε_i for ring samples was used.

Approximation of the actual strain curve of steel (Fig. 8) σ_i, ε_i, where $\sigma_i = \bar{\sigma}(1 + \bar{\varepsilon})\,\varepsilon_i = \ln(1 + \bar{\varepsilon})$, from σ_y, ε_y to start of neck formation $\sigma_{iu}, \varepsilon_{iu}$ can be calculated with the use of the following equation:

$$\sigma_i = \sigma_y \left(\frac{\varepsilon_i}{\varepsilon_y}\right)^m \tag{4}$$

where σ_y, $\varepsilon_y = \sigma_{0,2}$, $\varepsilon_{0,2}$, $m = 0.154253$.
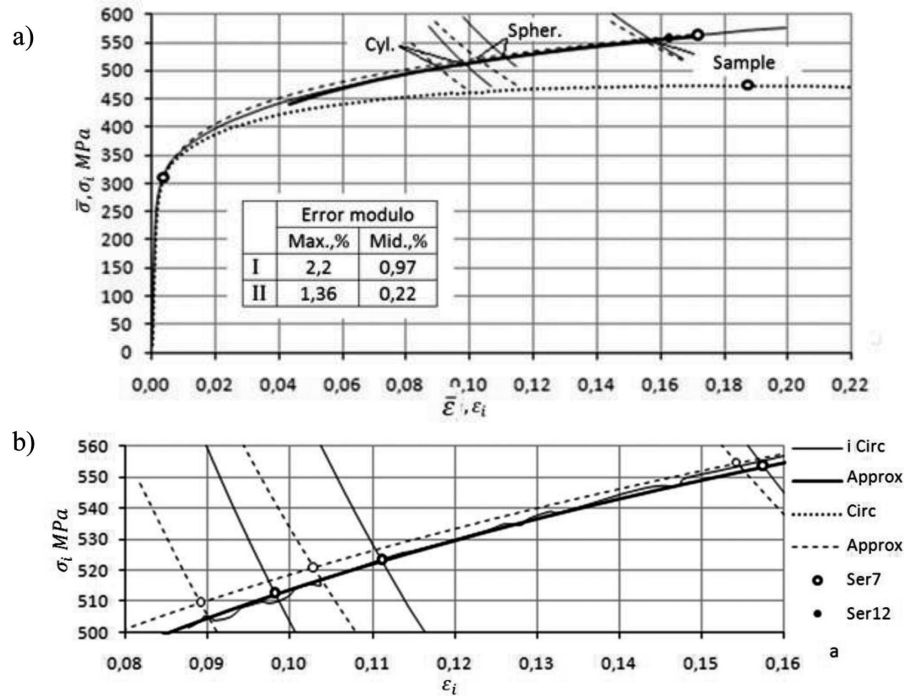

Fig. 8. Phase stable deformation sample made from thin-walled cylindrical and spherical shells that was loaded by internal pressure (a), scaled part curve (b)

Table 4.

Maximal values intensity of strain and stress stable deformation

	$\sigma_i = 740.0249\varepsilon_i^{0.154253}$		$\sigma_i = 87.17845\ln\varepsilon_i + 715.03$	
	I		II	
	ε_i	σ_i, MPa	ε_i	σ_i, MPa
Stretched sample	0.1542	554.6332	0.1574	553.8401
Spherical shell	0.1028	521.0067	0.1111	523.4706
Cylindrical shell	0.0892	509.7262	0.0982	512.7107

For thin-walled, cylindrical and spherical shells loaded by internal pressure with the initial radius equal to r_0, under large plastic deformations, the expression for the intensity of stress σ_i and logarithmic strain ε_i are actual for cylindrical shell:

$$\sigma_i = \frac{\sqrt{3}}{2}\frac{Pr}{s}, \quad \varepsilon_i = \frac{2}{\sqrt{3}}\ln\left(\frac{r}{r_0}\right) \tag{5}$$

where P − pressure; r_0 and r − initiate and mean radius shell; s – original wall thickness for spherical shell:

$$\sigma_i = \frac{Pr}{2s}, \quad \varepsilon_i = 2\ln\left(\frac{r}{r_0}\right) \tag{6}$$

When the loss of stability of the initial equilibrium shape of shells occurs, values r/r_0 for cylindrical and spherical shells can be obtained from the following expressions. [3]:

$$\frac{r}{r_0} = \exp\left[\frac{\sqrt{3}}{2}\left(\frac{m}{\sqrt{3}} - B\right)\right] = \exp\left(\frac{m}{2}\right) \tag{7}$$

$$\frac{r}{r_0} = \exp\left[\frac{1}{2}\left(\frac{2}{3}m - B\right)\right] = \exp\left(\frac{m}{3}\right) \tag{8}$$

where $m = 0.154253$.

The calculations show that for spherical shells relation r/r_0 is smaller than for cylindrical ones. Next, the dependence between the pressure P and the mean radius r for cylindrical and spherical shells is obtained [3]:
– cylindrical:

$$P = \frac{2}{\sqrt{3}}\frac{r_0 s_0}{r^2}A\left(B + \frac{2}{\sqrt{3}}\ln\frac{r}{r_0}\right)^m \tag{9}$$

– spherical:

$$P = \frac{2Ar_i^2 s_0}{r^3}\left(B + 2\ln\frac{r}{r_0}\right)^m \tag{10}$$

where s_0 – original wall thickness, $m = 0.154253$, B – constant.

It is worth pointing out that in the derivation of these calculations, relations were used obtained in the condition of incompressibility of the material for $\mu = 0.5$. For cylindrical shell formula: $r_0 s_0 = rs$, and for spherical shell approximation: $r_0^2 s_0 = r^2 s$. Thus it is possible to obtain pressure P^*, when loss of stability of equilibrium initial form shells occurs. Assuming that $B = 0$ the following expression is obtained for cylindrical shells:

$$P^* = \frac{2}{\sqrt{3}}\frac{As_0}{r_0\exp(m)}\left(\frac{m}{\sqrt{3}}\right)^m = 504.3225\frac{s_0}{r_0} \tag{11}$$

for spherical shells:

$$P^* = \frac{2As_0}{r_0 \exp(m)}\left(\frac{2m}{3}\right)^m = 893.1103\frac{s_0}{r_0} \tag{12}$$

Hence, $P^* = 28.413$ MPa and $P^* = 50.31607$ MPa for cylindrical and spherical shells, respectively. The spherical shell can withstand the pressure about 1.770911 times more than the cylindrical one. By using applying obtained results, it is possible to develop a practical application method of calculation of the mechanical properties of metal structures and criteria for their reliability. The results of experimental studies can be used as screening criteria during the examination of structures of cylindrical shape. After production of containers, as well as during their operation, their load span pressure P_s, which exceeds the working pressure P_w 1.5 times. If the container is built out of steel, where the ratio of tensile strength to yield strength ≥ 2, the pressure can be reduced to 1.5 times [6].

According to 1.9 [4], pipes of all types that work under pressure, must withstand a hydraulic pressure test that is calculated according to the formula given in [5]. Where, R – allowable stress equal to 40% of tensile strength for this steel, s – minimal (including minus tolerance) wall thickness of the pipe, mm and D – nominal outside diameter of the pipe, mm.
$D_c = D - s$; – calculated diameter of the pipe, mm.

$$\frac{s}{D} = \frac{6}{219} = 0.027.$$

Taking into account the nominal outside diameter (219 mm), minimum acceptable standard value of tensile strength (412 MPa) and nominal wall thickness (6 mm) the following values are obtained:

$$P_t = \frac{2sR}{D_p} = 9.285\,\text{MPa} \tag{13}$$

$$P_c = \frac{P_t}{1.5} = 6.19\,\text{MPa} \tag{14}$$

Taking into consideration the average value of tensile strength obtained in the samples cut in the circumferential direction (475.7 MPa), the values of 10.72 and 7.147 MPa, are obtained for P_t and P_c, respectively.

4. Conclusions

The article presents the stress-strain curve of the samples before the start of necking. The identical samples were cut in the circular direction. The

curves tension samples cut in the axial direction are characterized with a yield plateau. The diagrams show that the pipe in both the circumferential and axial directions indicates peculiar anisotropy. If the curve obtained for the circular samples moves to the right direction by 0.02, they approximately will be the same with the curves obtained from the axial direction. In the circular direction, the pipe deformed up to 2%, which is associated with its production.

Determination of the steady state during the deformation was carried out according to the method of calculation for thin-walled cylindrical and spherical shells, that was loaded by internal pressure.

Hence, $P^* = 28.413$ MPa and $P^* = 50.31607$ MPa for cylindrical and spherical shells, respectively. The spherical shell can withstand the pressure about 1.770911 times more than the cylindrical one.

The results of experimental studies can be used as screening criteria during the examination of structures of cylindrical shape.

Taking into account the nominal outside diameter (219 mm), minimum acceptable standard value of tensile strength (412 MPa) and nominal wall thickness (6 mm) the following values are obtained:

$$P_t = 9.285 \,\text{MPa}; \qquad P_c = 6.19 \,\text{MPa};$$

Taking into consideration the average value of tensile strength obtained in the samples cut in the circumferential direction (475.7 MPa), the values 10.72 and 7.147 MPa are obtained for P_t and P_c, respectively.

Acknowledgment

REFERENCES

[1] Borodavkin P.P., Edited by Sinykov A.M.: Strength of pipelines. Moskow, Nedra, 1984.
[2] Androno I.N., Kuzbogev A.S., Aginey R.V.: Resource of ground pipelines – I: Factors that constraining resource. Standard Test Methods, Ukhta, 2008, pp. 75-96.
[3] Malinin N.N.: Applied theory of plasticity and creep. Second Edition. Moskow, Mechanical engineering, 1975.

[4] GOST 8731-74 – Steel seamless hot rolled pipes. Technical requirements.
[5] GOST 3845-75 – Metal pipes. Method of hydraulic pressure test.
[6] Safety regulations 03-576-03 – The rules for design and safe operation of vessels that are working under pressure.
[7] Frost H.J., Ashby M.F.: Deformation-mechanism maps. Chelyabinsk, Metallurgy, 1989.
[8] Mildin A.M., Zelentsov D.G., Olevskiy V.I., Pletin V.V.: Developing the concept of prediction the mechanical properties of thin-walled shells. Eastern-European Journal of Enterprise Technologies, 2011, Vol. 1, No. 3, pp. 57-61.

Badanie naprężeń i odkształceń rury bezszwowej w stanie wyjściowym

S t r e s z c z e n i e

W pracy przedstawiono wyniki badań właściwości mechanicznych materiału z próbek wyciętych z rury bezszwowej na kierunku obwodowym i osiowym. Zaproponowano metodykę modelowania i szacowania stanu naprężenia i odkształcenia. Jest ona zgodna z metodologią stosowaną do analiz wytrzymałościowych cienkościennych cylindrycznych i sferycznych zbiorników poddanych ciśnieniu wewnętrznemu. W weryfikacji wyników wykorzystano wyniki badań doświadczalnych.